English Summary:

3.3 Coherence resonance

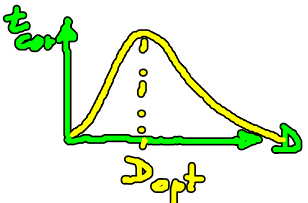

e.g. FHN model

3.4 Correlation time and power spectral density

Self-consistent mean-field approximation for VdP oscillator:

$$t_{corr}(D) = \frac{4}{\pi |\tilde{\varepsilon}(D)|}, \quad \tilde{\varepsilon}(D) = \frac{\varepsilon}{2}\left(1+\sqrt{1+\frac{2D^2}{\varepsilon^2\omega_0^2}}\right)$$

Half-width of power spectral peak: $\Delta\omega \approx \frac{|\tilde{\varepsilon}|}{2} = \frac{2}{\pi t_{corr}(D)}$

3.5 Kohärenzresonanz in anregbaren Systemen vom Typ I

3. Beispiel: SNIPER-Modell (Anregbarkeit Typ I)
(saddle-node infinite period bifurcation)

- knapp unterhalb einer globalen Bif. (Amplitude endl., $\omega \to 0$)
  Hopf: Amplitude $\to 0$, ω endl.
  ≡ SNIC ≙ saddle-node bif. on invariant cycle
  ≡ Sattel-Knoten-Bif. auf Grenzzyklus

Gang et al.: PRL 71, 807 (1993): Kohärenzresonanz erstmals
Arndt, Hövel, Hizanidis, Schöll: Eur. Phys. J. - ST 187, 77 (2010) mit delay

$$\dot{x} = x(1-x^2-y^2) + y(x-b) + D\xi(t)$$
$$\dot{y} = y(1-x^2-y^2) - x(x-b) + D\xi(t)$$

$D=0$:
$$\dot{r} = r(1-r^2)$$
$$\dot{\varphi} = b - r\cos\varphi$$

$x = r\cos\varphi$
$y = r\sin\varphi$

Fixp. (i) $r=0$ (instab. Fokus)
(ii) $r=1$, $\varphi = \arccos b$ (Sattelp. S)
(iii) $r=1$, $\varphi = -\arccos b$ (stab. Knoten N)
} ex. falls $b<1$

$b=1$: Sattel-Knoten-Bif. auf dem invarianter Kreis $r=1$
($r=1$, $\dot{r}=0$, $\dot{\varphi} = b-\cos\varphi$) $\dot{\varphi}=0$ für $\varphi=0$

$b>1$: Grenzzyklus $r=1$, $\int \frac{d\varphi}{b-\cos\varphi} = t \Rightarrow \varphi(t)$ analyt.

$$T = \frac{2\pi}{\sqrt{b^2-1}} \xrightarrow{b\to 1} \infty$$

Anregbares Regime : $b < 1$

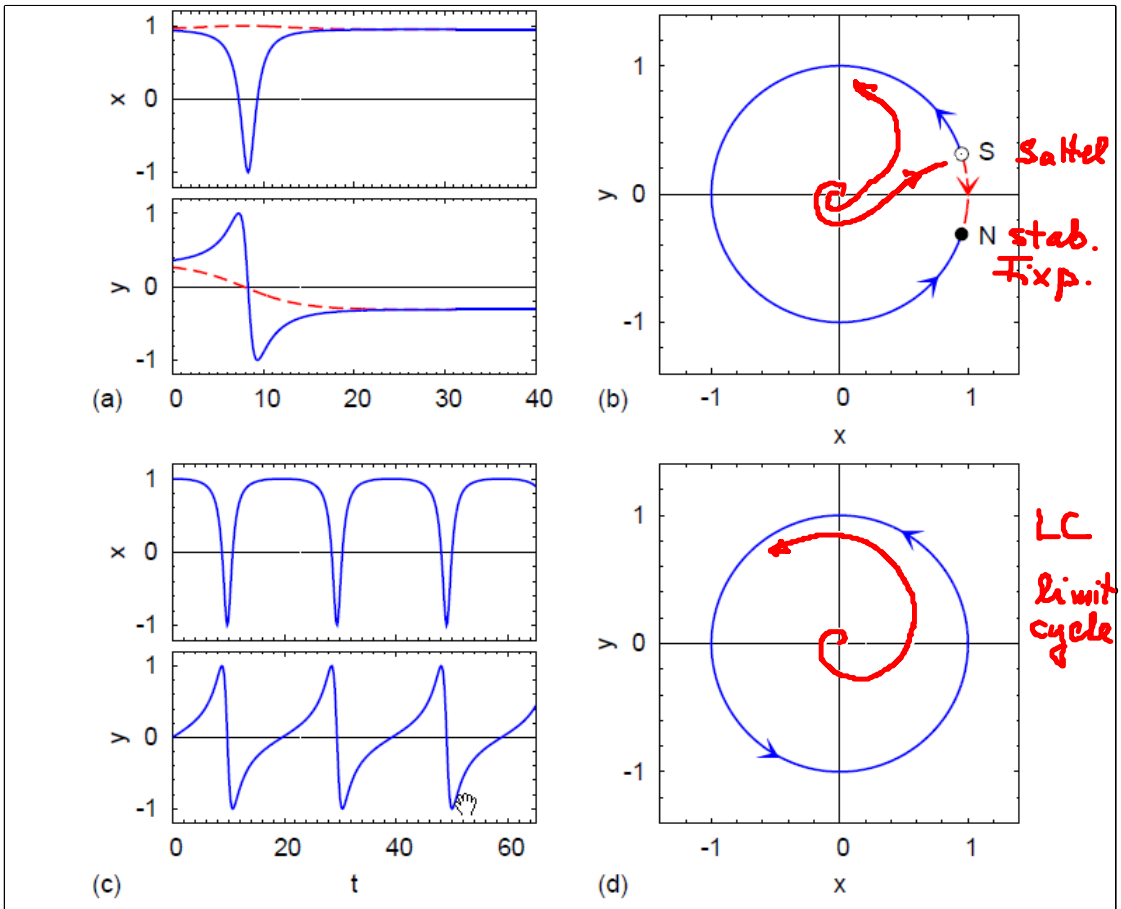

Aust et al. (2010)

= Schnelle S (für Anregung)

$b < 1$

$b > 1$

Fig. 1. (Color online) Time series (a),(c) and phase portraits (b),(d) of the analytic solutions of Eqs. (2). Panels (a),(b) refer to $b = 0.95 < 1$ with analytic solutions given by Eq. (7); full (blue) and broken (red) lines refer to two different initial conditions. Panels (c),(d) correspond to $b - 1.05 > 1$, see Eq. (8). ($K = D = 0$)

$D \neq 0$: Kohärenzresonanz

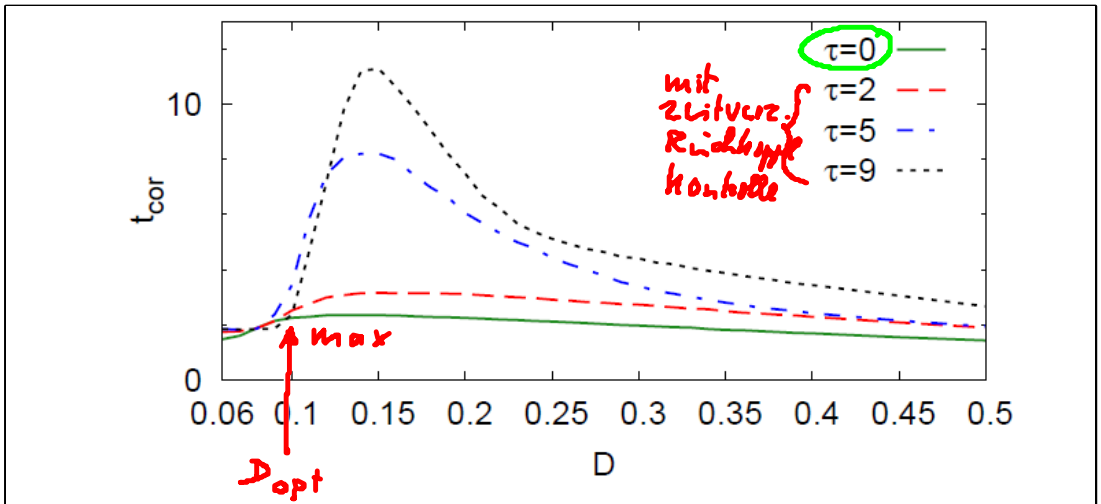

Aust et al (2010)

Fig. 4. (Color online) Correlation time in dependence on the noise intensity D for different time delays τ. The solid (green) curve corresponds to the uncontrolled system ($\tau = 0$). The dashed (red), dash-dotted (blue), and dotted (black) curves refer to values of $\tau = 2, 5$, and 9, respectively. Other parameters: $b = 0.95$ and $K = 0.25$.

Gang et al PRL (1993)

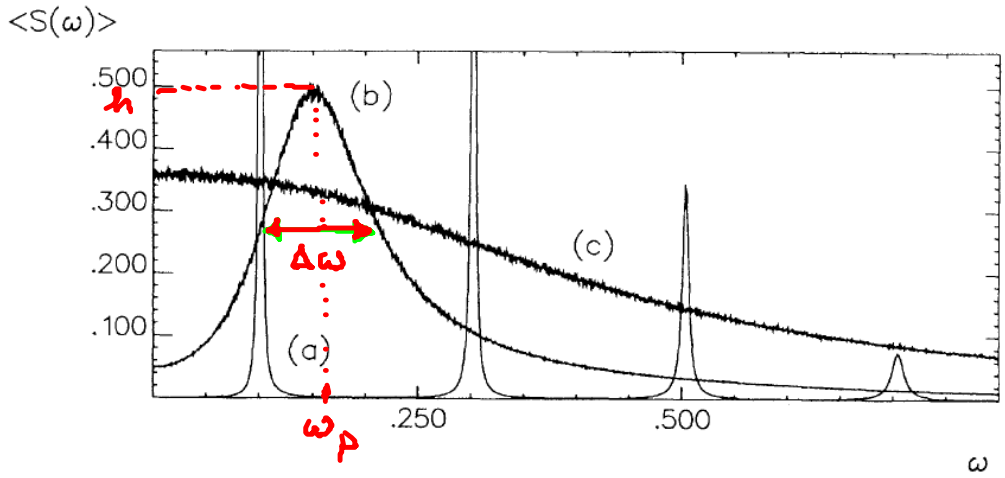

FIG. 1. The averaged power spectrum of $y(t)$ for $b=1.05$ and various D. A limit cycle exists for the deterministic system. (a) $D=0.00003$. (b) $D=0.05$. (c) $D=0.9$.

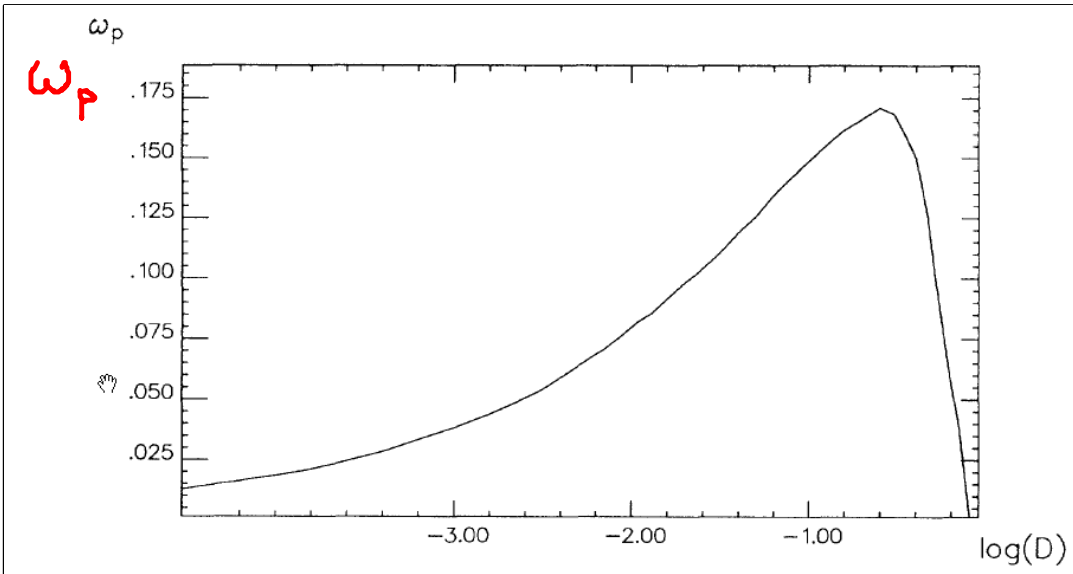

FIG. 3. The center frequency of the spectrum peak ω_p vs $\log(D)$ with $b=1$ (the same in Figs. 4 and 5).

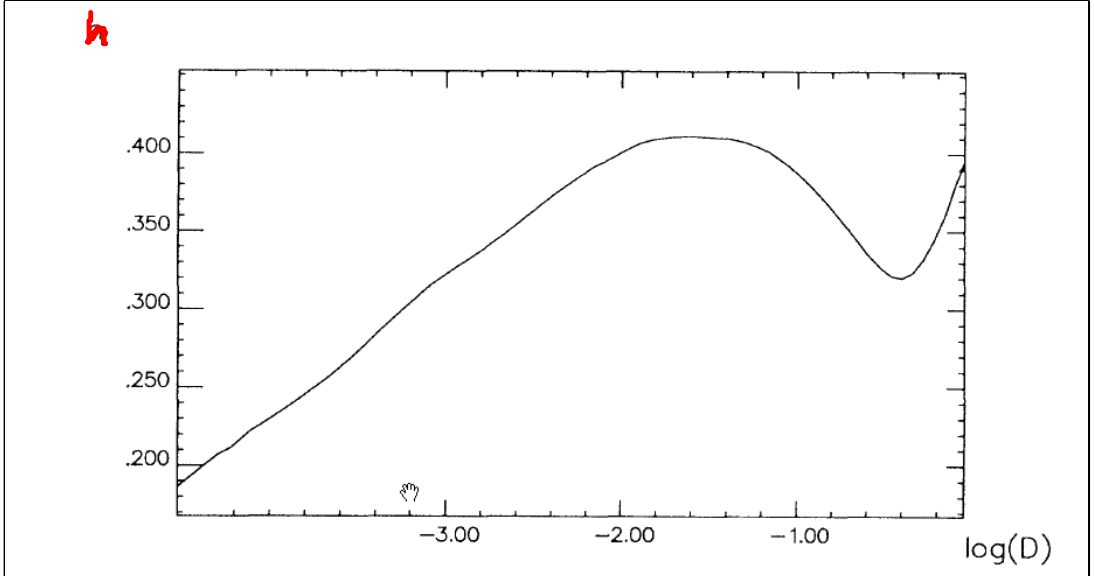

FIG. 4. The spectrum peak height h plotted against $\log(D)$. A resonancelike curve is obvious. However, h goes up again for very large D.

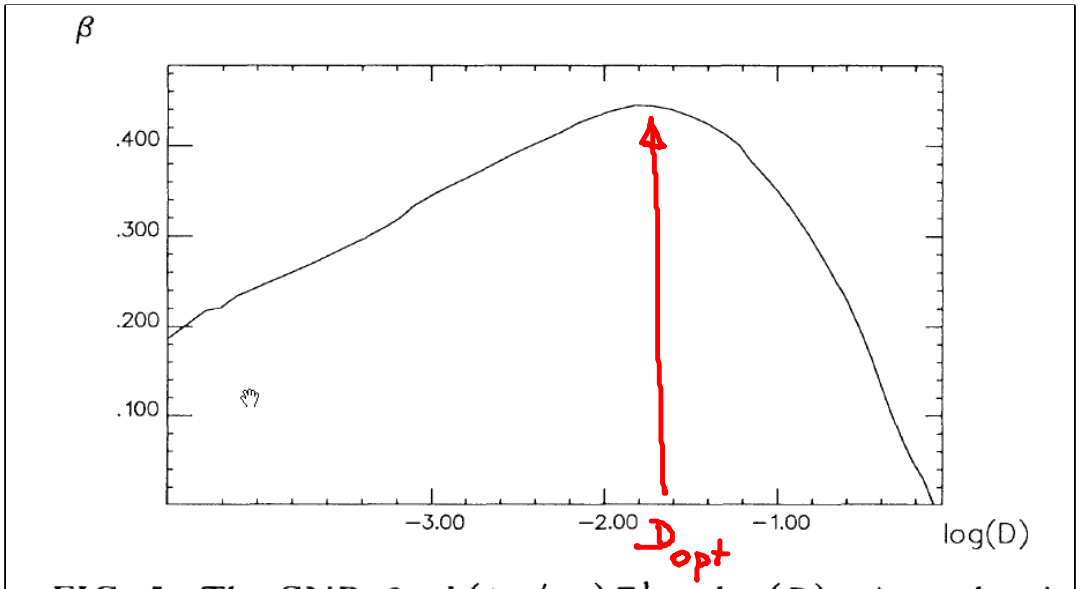

$$\beta = \frac{h}{\Delta\omega/\omega_p}$$

FIG. 5. The SNR $\beta = h(\Delta\omega/\omega_p)^{-1}$ vs $\log(D)$. A stochastic resonance maximum can be seen.

3.6 Kohärenzresonanz in nicht anregbaren Systemen

Kohärenzresonanz in der Nähe einer subkrit. Hopf-Bif.:

Geffert, Zakharova, Vüllings, Just, Schöll: Eur. Phys. J. B 87, 291 (14)
Ushakov, Wünsche, Henneberger, Khovanov, Schimansky-Geier, Zaks PRL 95, 123903 (2005) exp.+theor.
} gener. Stuart-Landau

Zakharova, Vadivasova, Anishchenko, Koseska, Kurths PRE 81, 011106 (2010)
Zakharova, Feoktistov, Vadivasova, Schöll: Eur. Phys. J. ST 222, 2481 (13)
Semenov, Feoktistov, Vadivasova, Schöll, Zakharova: Chaos 25, 033111 (15)
} gener. VdP osc.

Normalform einer superkrit. Hopf-Bif.:

$$\dot z = (\lambda + i\omega - |z|^2)\, z + \sqrt{2D}\,\xi(t) \qquad z = re^{i\varphi} \in \mathbb{C}$$

Stuart-Landau-Oszillator

$$\dot r = (\lambda - r^2)\, r, \qquad \dot\varphi = \omega \quad \Rightarrow \varphi = \omega t$$

D=0 : Fixp. $z=0$
Eigenwert $\lambda + i\omega$ ⟶ $\lambda < 0$: stabiler Fokus
$\lambda > 0$: instab. Fokus + stabiler Grenzzyklus $r = \sqrt{\lambda}$
Hopf-Bif. bei $\lambda = 0$

Normalform einer subkrit. Hopf-Bif.:

$$\dot z = (\lambda + i\omega + s|z|^2 - |z|^4)\, z + \sqrt{2D}\,\xi(t) \qquad s = 1$$

verallgem. Stuart-Landau-Osz.

D=0 : $\dot r = (\lambda + s r^2 - r^4)\, r$, $\dot\varphi = \omega$ Fixp. $r = 0$ stabil für $\lambda < 0$

Grenzzyklen ($r \neq 0$): $r^4 - s r^2 - \lambda = 0 \Rightarrow r^2 = \frac{s}{2}\left(1 \pm \underbrace{\sqrt{1 + \frac{4\lambda}{s^2}}}_{>0 \text{ für } \lambda > -\frac{s^2}{4}}\right)$ (Klammerausdruck > 0)

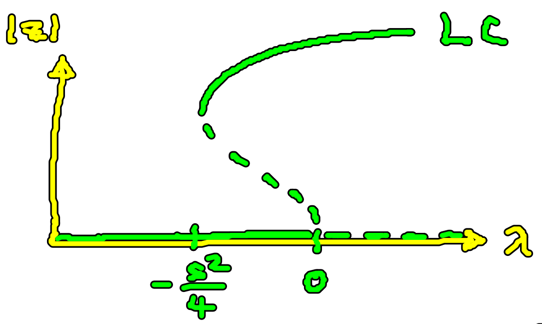

Sattel-Knoten-Bif. eines stabilen u. instab. LC bei $\lambda = -\frac{s^2}{4}$

$z(t) = r e^{i\omega t}$

Bistabilität zwischen Fixp. $z = 0$ und LC mit $r^2 = \frac{s}{2}\left(1 + \sqrt{1 + \frac{4\lambda}{s^2}}\right)$
für $-\frac{s^2}{4} \leq \lambda \leq 0$

$D \neq 0$: stationäre Lösung der FP-gl.

$$P(r) = N r \exp\left\{\frac{r^2}{D}\left(\frac{s}{2} + \frac{sr^2}{3} - \frac{r^4}{6}\right)\right\}$$

N: wegen Normierung in Polarkoord.

$\frac{U(r)}{D}$, $-U'(r) = A(r)$ Drift

Amplituden-Wahrscheinl.verteilung (Radialsymm.)

$\iint p(r,\varphi)\, r\, dr\, d\varphi = \int p\, 2\pi r\, dr$

$P(r)$ Amplituden-Wahrscheinl.dichte für Ring mit Radius r

Stochast. Bifurkation : $P(r)$ unimodal → bimodal

(Phänomenolog. Bif. = P-Bif.)

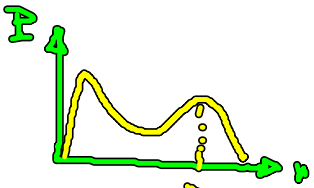

Übergang: Wendepkt. v. U mit hor. Tang.

rauschinduz. Dse. im Ursprung

rauschinduz. stoch. LC bei r_0

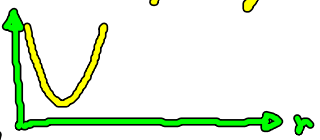

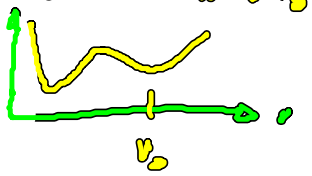

$$(\ln P)' = 0 : -\frac{D}{r} - \lambda r - s r^3 + r^5 = 0$$

$$(\ln P)'' = 0 : \frac{D}{r^2} - \lambda - 3 s r^2 + 5 r^4 = 0$$

$$\Rightarrow r^2 = -\frac{9D + \lambda s}{6\lambda + 2s^2} > 0$$

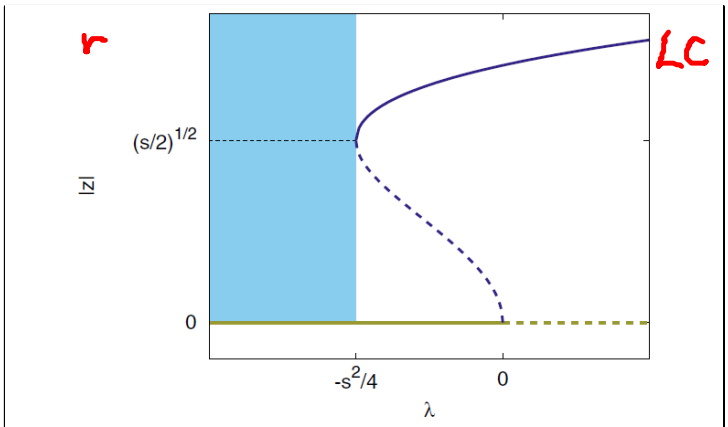

Fig. 1. The bifurcation diagram of the deterministic system without time delay, equation (1) for $K = 0$ and $D = 0$, in the subcritical regime $s > 0$. Bronze (grey): trivial fixed point (solid: stable, dashed: unstable), blue (black): periodic orbit (solid: stable, dashed: unstable), dotted line: location of the saddle-node bifurcation of periodic orbits. The shaded region is the parameter region of interest for coherence resonance.

Gelfert et al (2014)

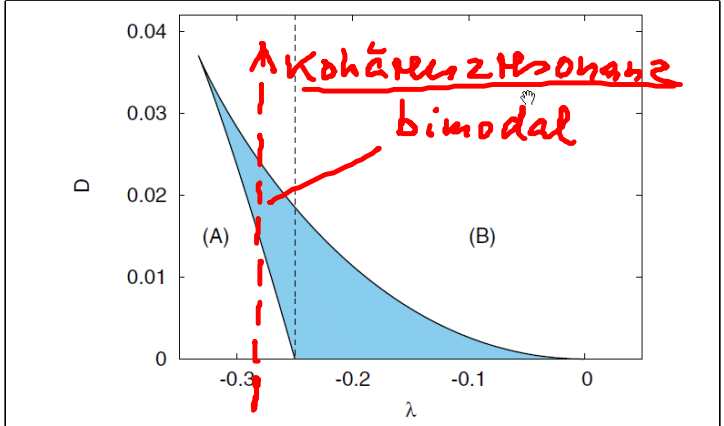

Fig. 2. Stochastic bifurcation diagram of the stochastic differential equation without delay equation (1), corresponding to equation (5) for $s = 1$. The blue shaded area denotes the parameter values, where the probability distribution has a bimodal shape. The dashed line shows the border between the deterministic monostable (A) and the deterministic bistable (B) regime.

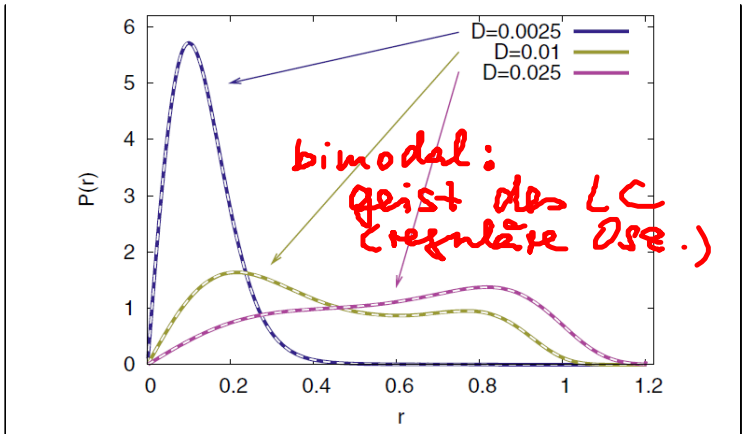

Fig. 3. Stationary amplitude probability distribution of the stochastic delay differential equation for $\omega = 2\pi$, $\lambda = 0.18$, $s = 1$, $\tau = 0.25$, $K = 0.5$ and three values of the noise strength D as obtained from numerical simulations of equation (1) (solid lines). Dashed lines (white) show the respective result of an analytical approximation scheme (Eq. (9)). The analytical approximation is in excellent agreement with the simulation results.

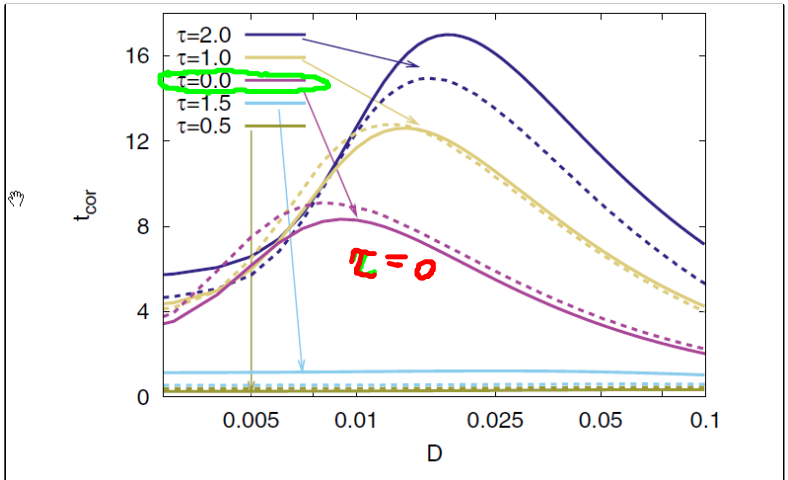

Kennel. zeit

Fig. 8. Influence of the time delay on the correlation time t_{cor}. The dashed lines correspond to numerical simulations of equation (1), the solid lines show the approximation, calculated from equation (27) with $\ell = \ell' = 0$. Parameters: $\omega = 2\pi$, $\lambda = -0.26$, $K = 0.5$, $s = 1$.

Spektrale Resonanzkurve

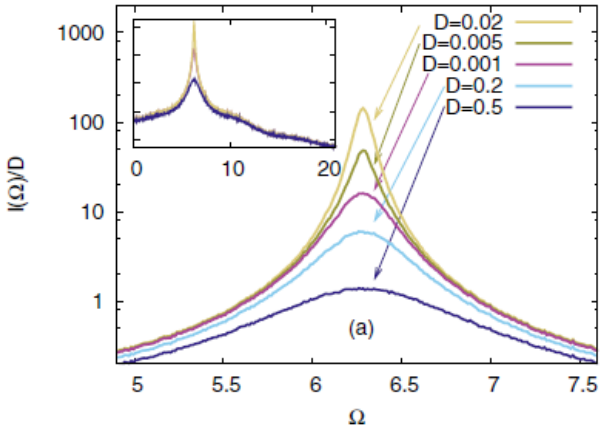

$\lambda = -0.26$

$\lambda = -0.35$

Fig. 6. Normalised power spectral density $I(\Omega)/D$ in the vicinity of the central peak at $\Omega = 2\pi$, as obtained from a numerical simulation of equation (1) for increasing values of the noise intensity D, $\tau = 1.0$, $\omega = 2\pi$, $K = 0.5$, $s = 1$ and two different values of λ (a) $\lambda = -0.26$, (b) $\lambda = -0.35$ (see Fig. 5). The insets show the structure of the power spectral densities for $D = 0.001$, $D = 0.01$ and $D = 0.1$ on a larger scale.

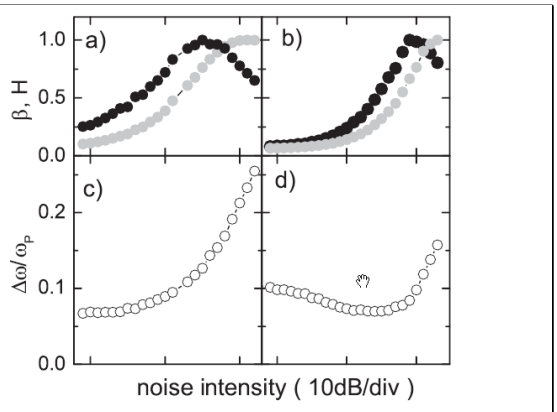

FIG. 2. Peak height (gray dots), normalized width (open dots), and signal-to-noise ratio (black dots) versus noise intensity as deduced from the power spectra by Lorentzian fits. Note the log scale. (a),(c) Supercritical bifurcation, (b), (d) Subcritical bifurcation. Maxima of curves are normalized to unity.

Exp.
(Mahdavi et al 2005)

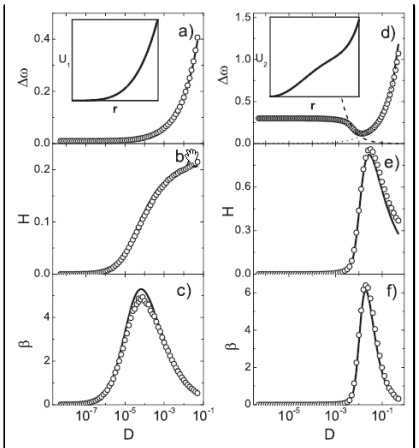

FIG. 3. Width (Δ_ω), peak height (H), and signal-to-noise ratio (β) versus noise intensity (D) as obtained from the theoretical analysis. Left column (a)–(c) Supercritical bifurcation ($F = F_1$). Right column (d)–(f) Subcritical bifurcation ($F = F_2$). Symbols "○" represent the numerical solution of (2), lines are obtained from the analytical treatment. Insets: Shape of the potentials $U_1(r)$ and $U_2(r)$. Dashed lines in (d) show the asymptotic behavior D^{-1} and $D^{2/3}$, respectively (see text for details).

theor.